UNIVERSITY OF MINNESOTA
ST. ANTHONY FALLS HYDRAULIC LABORATORY

Project Report No. 225

HYDROMECHANICS OF VARIABLE SPEED TURBINES

by

Cesar Farell, Javier Arroyave,
Nicholas Cruz, and John S. Gulliver

Prepared for

STATE OF MINNESOTA
DEPARTMENT OF NATURAL RESOURCES
St. Paul, Minnesota

August, 1983
Minneapolis, Minnesota

University of Minnesota
St. Anthony Falls Hydraulic Laboratory

Project Report No. 225

HYDROMECHANICS OF VARIABLE SPEED TURBINES

by

Cesar Farell, Javier Arroyave,

Nicholas Cruz, and John S. Gulliver

Prepared for

STATE OF MINNESOTA
DEPARTMENT OF NATURAL RESOURCES
St. Paul, Minnesota

August, 1983

ACKNOWLEDGEMENTS

This study was performed under the general supervision of Dr. Roger E.A. Arndt, Director of the St. Anthony Falls Hydraulic Laboratory, University of Minnesota.

TABLE OF CONTENTS

LIST OF FIGURES

I. INTRODUCTION

The increased use of wind-driven generators in the last few years has resulted in special generator designs which operate at varying speed and frequency, utilizing static inverters for conversion of direct to alternating current. The potential application of this emerging technology to hydropower production schemes has recently received considerable attention, as witnessed, for example, by the recent DOE-EPRI (1983) workshop on applications of variable-speed generators in hydropower. Typically, a variable-speed hydroelectric scheme would consist essentially of the turbine, a synchronous generator (variable speed and frequency), a rectifier for the generator output, an inverter at the powerhouse and alternating current transmission, or direct current transmission, and an inverter at the substation. Regardless of the speed variations, the inverters have the ability to maintain virtually constant frequency and voltage for any given load.

While rectifiers and inverters are added elements in variable-speed schemes, certain simplifications and cost reductions may result in other areas, which must be taken into account in potential cost benefit studies. Although the purpose of the present report is to discuss hydromechanical aspects of variable-speed turbine operation, a few generator and control features are briefly touched upon here to give a more general perspective of the overall problem. First, since the generator output is rectified in a variable-speed scheme, the number of generator poles can be optimized to simplify generator construction, without regard for the electrical load. Second, because of less severe requirements on voltage wave-forms, simplifications may also be possible in both pole and stator windings. Third, for variable head units, it may be possible to match the turbine rating with a smaller generator by running at variable speed, because a smaller output range results from variable speed operation, and

more flexibility is then available to place the design head within the head range. Fourth, waterhammer and governing problems are considerably simplified, resulting in savings in space, equipment, and maintenance. For low-head, low-power applications in particular, constant-speed turbine-generator units generally have low inertia constants which require the use of flywheels, with or without speed reducers. For variable speed operation, the complication of control schemes which make up a large proportion of the total cost for smaller units is considerably reduced or eliminated altogether. Continuously acting speed control and flywheels are not necessary, although some limited speed control may be necessary to provide operational limits and load sharing between units.

For additional discussion of generator and inverter technology, the reader is referred to Nair (1982) and the DOE-EPRI (1983) workshop. It appears from the workshop presentations and results that the electric field is being actively investigated and there is a need for parallel research on the hydromechanical aspects of the turbines. Several types of variable speed generators are presently being examined (including in particular doubly fed machines). Inverter technology is advancing rapidly, and research and development efforts for best conversion methods for wind-turbine, small-hydro, and existing large-hydro power generation are under review.

The present report focuses on hydromechanical aspects of variable-speed turbine operation. Possible applications and advantages from a hydromechanics point of view are briefly discussed in the next section, similarity conditions are analyzed in section III, applications of similarity laws to variable-speed turbine performance estimates are presented in section IV, and some theoretical calculations for axial flow (propeller) turbines are discussed in section V. Finally, conclusions and ideas for future research are briefly reviewed in section VI.

II. POSSIBLE APPLICATIONS OF THE VARIABLE-SPEED TURBINE

Possible variable-speed turbine applications and benefits depend on the mode of plant operation, and potential cost-benefit analyses require the definition of operation scenarios. Sheldon (1983) and Alexander (1983) have recently performed analyses of energy and water gains for Francis turbines under various conditions of operation, using model test performance data for specific turbines already installed. In principle, allowing for variation of the turbine speed should result in the following advantages:

a) Improved performance at off-design heads and improved range of operating heads. Low-head propeller turbines in particular can experience a very wide range of operating head as a percent of design head.

b) Improved performance at off-design discharges and improved range of operating discharges.

c) Improved performance for pump-turbine units. Here if the rotational speed is to be the same for both turbine and pump operations, some sacrifice in efficiency in either or both modes is generally necessary. Pump-turbine applications involve usually high heads and relatively large head variations, and require radial or mixed flow machines. Wislicenus (1979) has pointed out that axial-flow machines, except for their low operating head, are theoretically more attractive as pump-turbines than radial-flow machines because they operate near optimum efficiency at a given rotational speed in both the pumping and turbining modes. The use of multi-stage axial flow units has been suggested by Wislicenus as a possible improvement. Obviously, variable-speed operation of Francis units should also be examined in this regard because peak efficiency can be achieved without the expensive multi-stage option.

Determination of the potential benefits of the variable speed turbine depends obviously on quantifying the improvements in performance. The results of Sheldon (1983) for three specific Francis units (n_s = 24.5, 44.7, and 56.1 in English units) show that variable speed provides small increases in energy production relative to the water used. For three scenarios with heads varying ±50 percent from the best-efficiency head, Sheldon considered machines operating at best possible efficiency, at constant or maximum possible power, and at constant or maximum possible discharge. For the best possible efficiency case, an energy increase of 3.5 percent and water saving of 0.1 percent resulted for n_s = 24.5 , while for n_s = 56.1 , the energy increase was smaller, 1.6 percent, but the water saving of 4.9 percent was larger.

These results apply to the specific turbines analyzed. Other units may behave differently, and it might be possible that turbine design optimization for variable speed may result in larger gains. As Alexander (1983) has pointed out, the turbines he used in his study (one of which coincides with one of the units in Sheldon's (1983) analysis) were built to provide a wide operating range rather than maximum peak efficiency. Variable speed turbines designed for highest efficiency should show greater improvements in energy recovery. For fixed-blade propeller turbines, which have very narrow operational ranges as a percent of full load (see Fig. 1), the results could be very different, in particular if large relative head variations occur. Since fixed-blade propeller turbines are much less costly than Kaplan turbines, their potential cost benefits should be examined in detail.

Development of software for producing benefit analyses relative to a set of specific scenarios require that detailed turbine data be available. These data are generally lacking, on the one hand because of the proprietary nature of the manufacturer's design information, and on the other because many developments in the design of small scale units are relatively recent. Sometimes the available performance data does not cover the entire range of possible variable-speed operation. Thus, additional data appears to be needed, as would be obtained in a turbine test stand using scale models. In the following, the nature of the required data is illustrated in the light of several specific analyses.

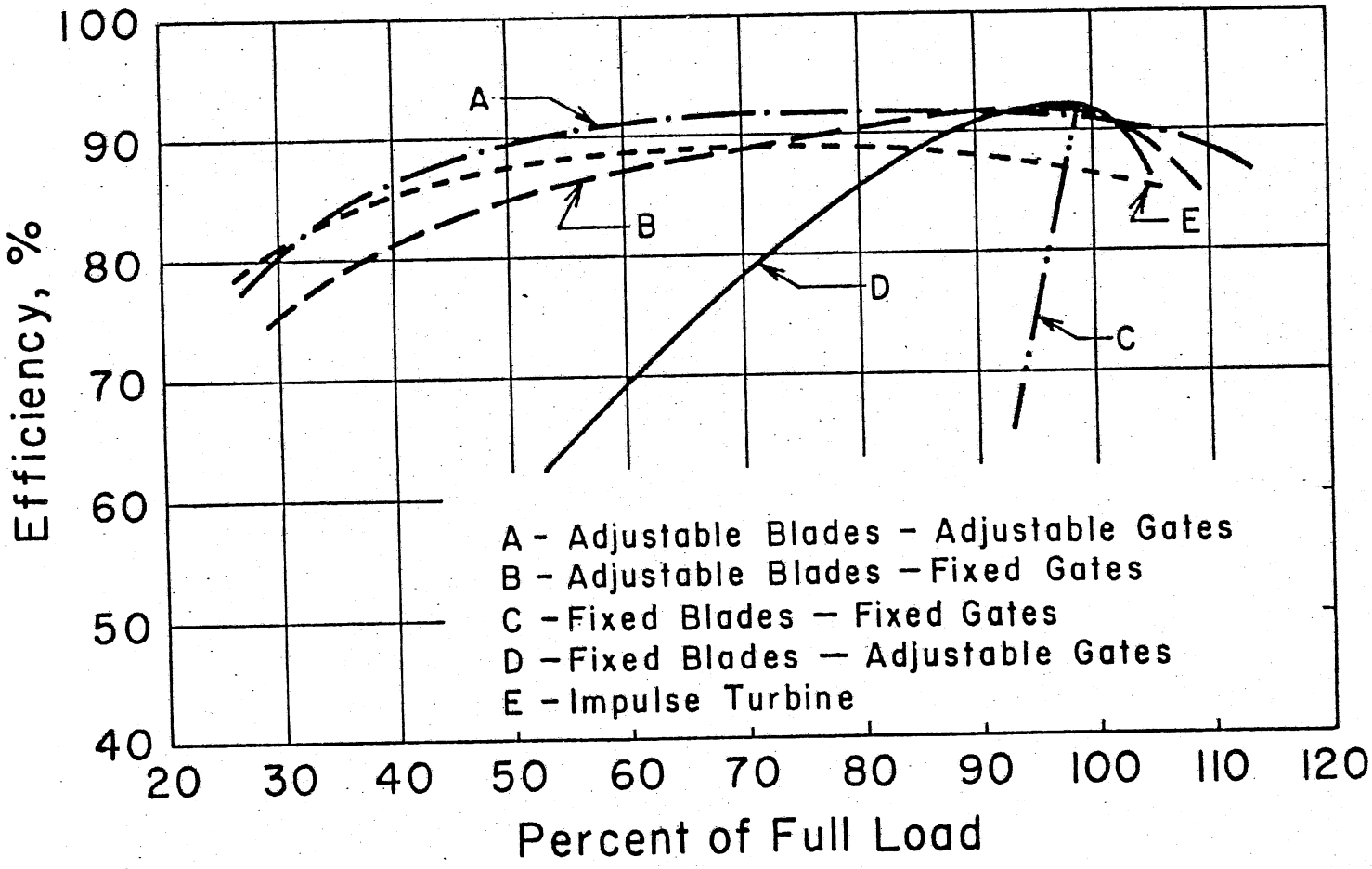

Fig. 1. Turbine efficiency as a function of percent of full load. Constant speed operation.

III. SIMILARITY CONDITIONS AND OPERATING CHARACTERISTICS

The grouping of parameters brought about by dimensional analysis permits the writing of a physical relationship in terms of fewer dimensionless quantities (π numbers) representing ratios of significant forces for the problem. This provides a method to extrapolate model test data to prototype situations by equating corresponding dimensionless numbers. As applied to hydraulic machinery, similarity considerations provide, futhermore, an answer to the following important question: Given test data on the performance characteristics of a certain type of machine under certain operating conditions, what can be said about the performance characteristics of the same machine, or of a geometrically similar machine under different operating conditions? Similarity considerations provide, in addition, a means of cataloguing machine types and thus aid in the selection of the type suitable for a particular set of conditions.

The problem of similarity of flow conditons can be summarized as follows: Under what conditions will geometrically similar flow patterns with proportional velocities and accelerations occur around or within geometrically similar bodies? Obviously, the forces acting on corresponding fluid masses must be proportionally related, as are the kinematic quantities, so as to insure that the fluid will follow geometrically similar paths. An answer to this question can be obtained by examining the fundamental laws of motion and identifying the relevant forces. While these laws cannot yet be used predict theoretically the flow conditions in a machine with unknown performance characteristics, the information they provide on forces and boundary conditions enables the determination of an answer to the similitude problem.

For geometrically similar machines, kinematic similarity requires that the ratio $Q/\Omega D^3$ be the same for model and prototype. Here Q is the turbine discharge, Ω is the rotational speed in radians per second ($\Omega = 2\pi n/60$, where n = rotational speed in revolutions per minute),

and D is a typical runner diameter. In the rotating coordinate system this ratio represents also the ratio between inertial and centrifugal forces, or equivalently the ratio between kinetic energy and the potential energy of the centrifugal force.

The condition $Q/\Omega D^3$ = constant is actually sufficient for similarity. The dynamic similarity condition $gH/\Omega^2 D^2$ = constant follows from the basic laws and permits calculation of the head H for similar operating conditions. For brevity, energy losses and volumetric efficiencies have been left out of the discussion as presented here. Equality of hydraulic, volumetric, and mechanical efficiencies is necessary for strict similarity. Departures from this equality produce scale effects, a discussion of which can be found in Arndt, Farell, and Wetzel (in press).

III.1. Specific Speed

Similar flow conditions are ensured by the constancy of the ratio $Q/\Omega D^3$, which implies constancy of the ratio $gH/\Omega^2 D^2$. In other words

$$\frac{gH}{\Omega^2 D^2} = f\left(\frac{Q}{\Omega D^3}\right) \tag{1}$$

This relationship can also be written in terms of a third dimensionless number which does not involve the representative dimension D of the machine, and which can replace either of the two arguments in Eq. (1). Such a number can be obtained by appropriate multiplication of powers of the dimensionless numbers in Eq. (1):

$$N_{S_Q} = \left(\frac{Q}{\Omega D^3}\right)^{1/2} \left(\frac{\Omega^2 D^2}{gH}\right)^{3/4} = \frac{\Omega Q^{1/2}}{(gH)^{3/4}} \tag{2}$$

This dimensionless number is called the specific speed. For hydraulic turbines, however, the definition of the specific speed is based on the power P delivered by the turbine as a variable, instead of on the flow rate Q. The corresponding dimensionless number to ensure kinematic similarity for P is $P/\rho\Omega^3 D^5$, which is a function of $gH/\Omega^2 D^2$. Eliminating D between these two numbers one gets

$$N_S = \frac{\Omega (P/\rho)^{1/2}}{(gH)^{5/4}} \tag{3}$$

The two specific speeds are related by

$$N_s = \sqrt{\eta}\, N_{s_Q} \tag{4}$$

which is obtained making use of the equation $P = \eta\gamma QH$. If we choose N_s as the independent variable in these relationships, then all other dimensionless combinations can be expressed as functions of N_s.

The specific speed describes a specific combination of operating conditions that ensures similar flows in geometrically similar machines. It has thus attached to it a specific value of efficiency, η (assumed approximately constant for similar flow conditions regardless of size). It is customary to label each series of geometrically similar turbines by the value of N_s which gives maximum η for the series. Unless otherwise stated, this is the N_s value referred to when the terminology specific speed is used. The value of N_s thus defined permits the classification of turbines according to efficiency. Each geometric design has a range of N_s values where it can be used with only one value corresponding to peak efficiency. Figure 2 shows the peak efficiency of various types of turbines as a function of specific speed.

The N_s, as it was defined here, is dimensionless. It is common practice to drop g and ρ from the definition and define n_s as

$$n_s = \frac{n\sqrt{P}}{H^{5/4}} \tag{5}$$

with n in rpm. In English units, the units of P are horsepower, and the units of H are feet. In metric units, the unit of P is either the metric horsepower or the kilowatt, and the unit of H is the meter. The relationships of these three definitions of n_s to the dimensionless N_s are:

$$\begin{aligned} n_s &= 43.5\, N_s \quad \text{(English units)} \\ n_s &= 193.1\, N_s \quad \text{(Metric units using metric horsepower)} \\ n_s &= 166\, N_s \quad \text{(Metric units using KW for power)} \end{aligned} \tag{6}$$

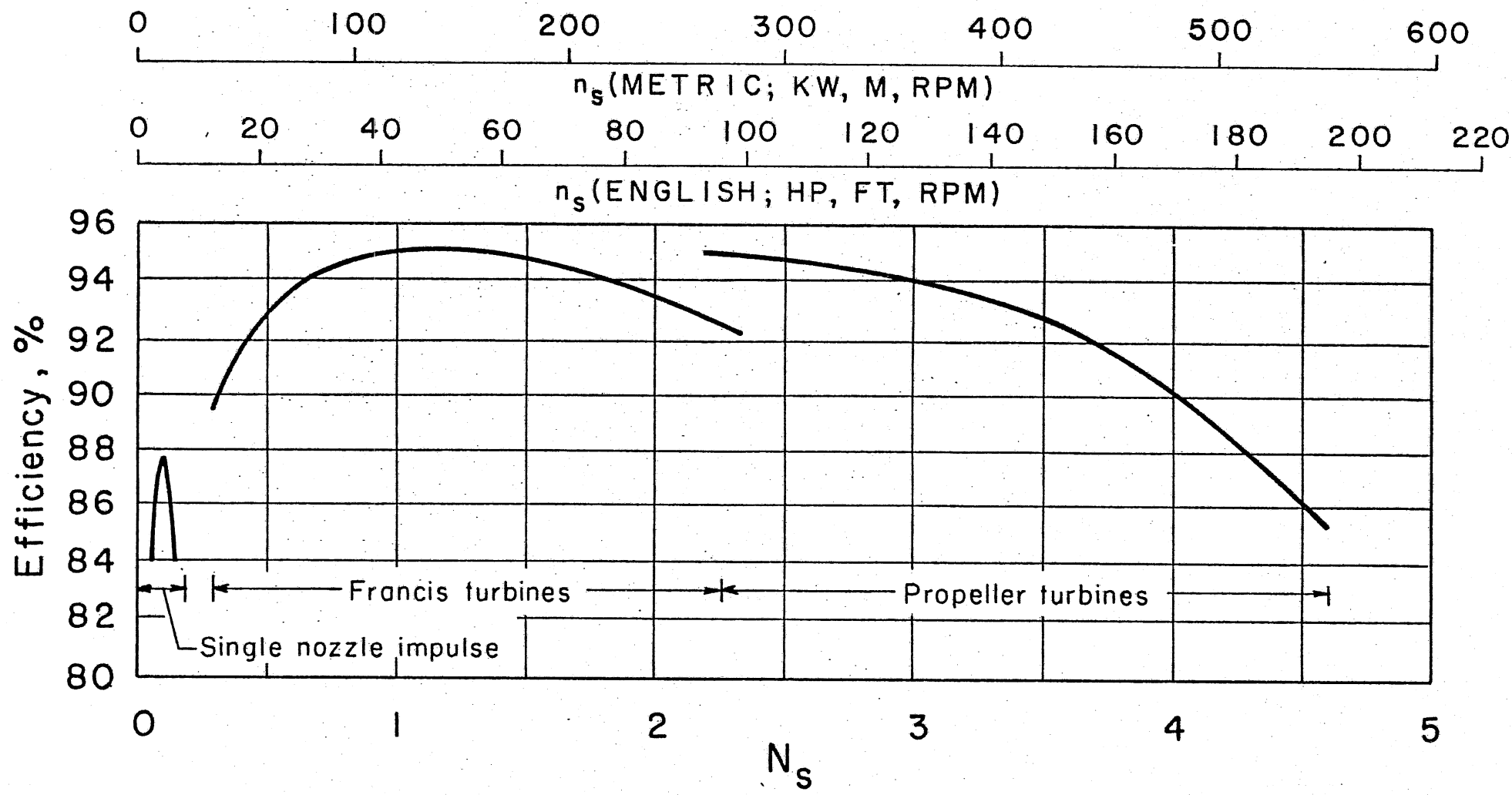

Fig. 2. Maximum efficiencies and turbine ranges as functions of specific speed.

Abcissa axes showing metric and English units have been added to Fig. 2 for convenience.

III.2. Performance Curves and Characteristic Diagrams

Typical head-discharge-efficiency performance curves for constant speed operation for a fixed-blade, fixed-gate axial turbine are given in Fig. 3. These curves show operating conditions of the turbine at points other than the design or best efficiency point. From such a diagram it is possible to obtain operating conditions for the turbine at speeds other than the design speed by using the two similarity conditions, which give

$$\frac{Q_1}{\Omega_1} = \frac{Q_2}{\Omega_2} \quad \text{and} \quad \frac{H_1}{\Omega_1^2} = \frac{H_2}{\Omega_2^2} \tag{7}$$

In addition, the efficiencies are assumed to be equal as well, $\eta_1 = \eta_2$.

In general, for a variable-gate turbine, a characteristic diagram can be prepared with the dimensionless parameters in Eq. (1) as coordinates and the gate opening as parameter. Curves of constant efficiency can be shown on the diagram, which is then known as a performance hill diagram. Alternately, one can use the best efficiency vales of the parameters on the coordinate axes to convert the diagram to a percent discharge-percent head diagram. Power can also be used in one of the coordinate axes or as an additional parameter (in dimensionless form). For a Kaplan turbine, the blade angle is an additional parameter.

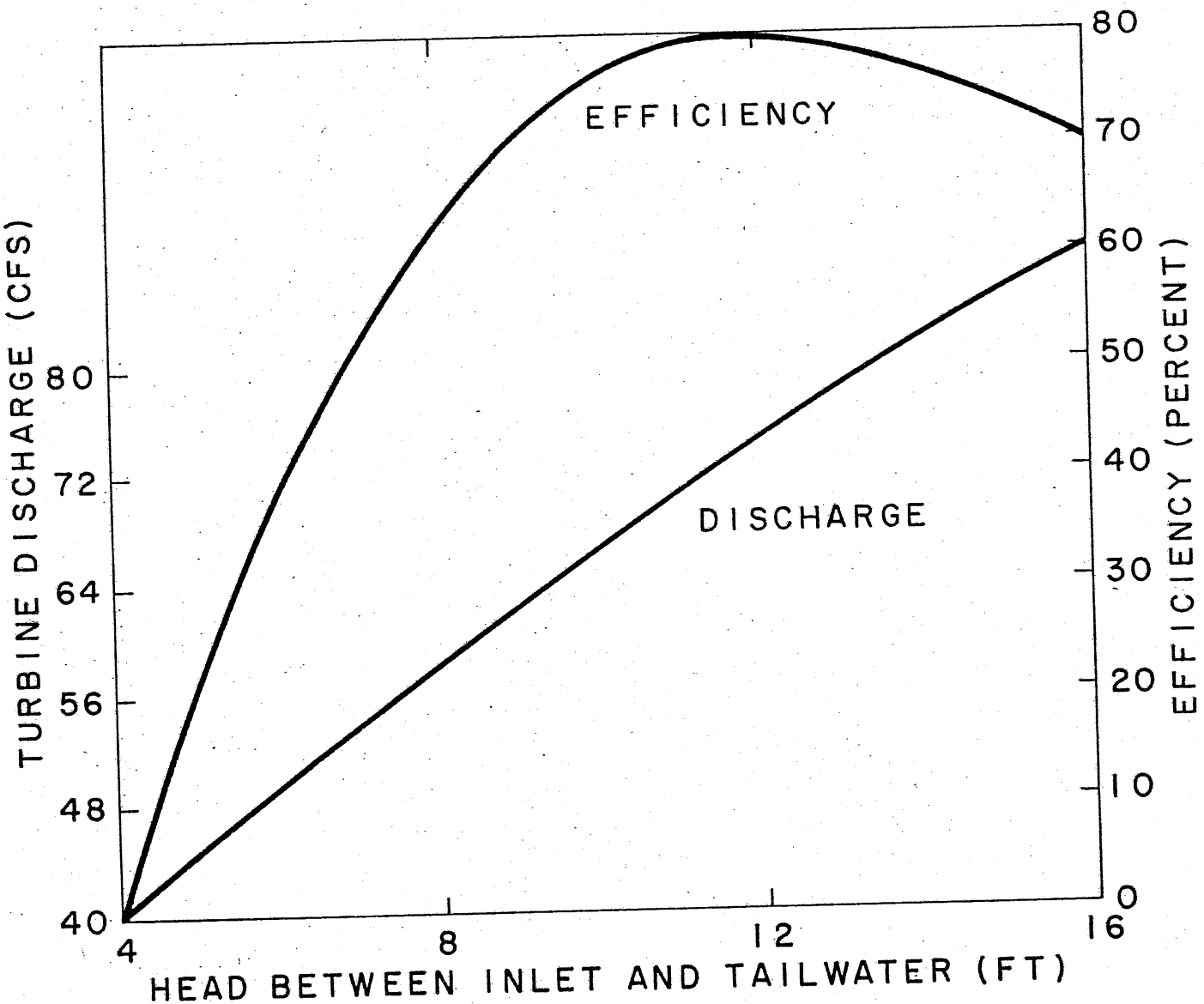

Fig. 3. Typical head-discharge-efficiency curves for an axial flow turbine.

IV. VARIABLE-SPEED TURBINE PERFORMANCE AT CONSTANT HEAD

Variable-speed performance diagrams at constant head for two small axial-flow turbines with fixed vanes and blades, A_1 and A_2, an axial pump used as a turbine, P_1, three Francis turbines, F_1, F_2, and F_3, a pump turbine, T_1, and a Kaplan turbine, K_1, were obtained from information supplied by manufacturers or available in the literature. The original information was in different form for the various cases investigated, and the processing of the data differed for each turbine, as outlined below. The following table gives the specific speeds of the turbines analyzed:

	N_s	n_s(kW,m,rpm)	n_s(hp,ft,rpm)
A_1	1.61	267	70
A_2	2.65	440	115
P_1	2.68	444	116
F_1	0.51	84	22
F_2	0.81	134	35
F_3	1.43	237	62
T_1	0.76	127	33
K_1	3.26	542	142

On the H-Q plane, if the fixed-gate characteristic curve of a turbine is known for a given speed, the similarity laws can be used as explained in the preceding section to obtain the characteristic curves at other speeds. Generally, the form of this H-Q curve is as shown in Fig. 4. If the turbine fixed-gate, H-Q curve at constant speed is steeper than the similarity parabola linking equal-efficiency points, then it is seen that for

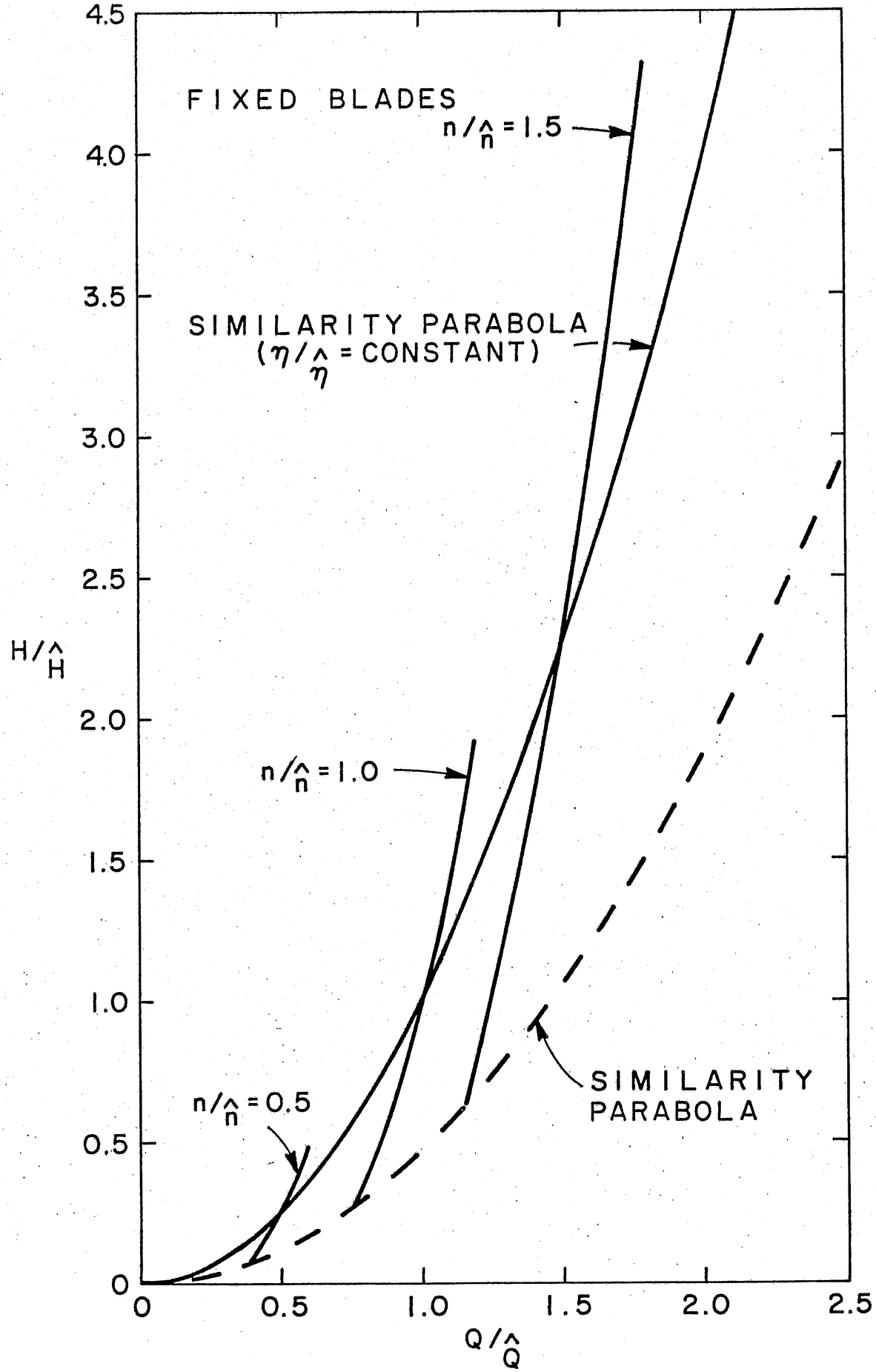

Fig. 4. Sketch of fixed-gate characteristic curves on H-Q plane for different speeds. ($\hat{H}$, $\hat{Q}$, $\hat{\eta}$: best-efficiency values)

constant H, Q will be an increasing function of n. The opposite is true if the similarity parabola is steeper than the H-Q curve. Both cases actually can occur, as shown later on.

A computer program was prepared to carry out numerically the similarity calculations indicated in the preceding paragraph. Original values from the known performance curves of the turbine at constant speed were stored in discrete form, for small head increments ΔH, in reference column matrices QREF(I), HREF(I), PREF(I), and EFF(I). The values generated using the similarity relationships for different turbine speeds were stored in matrices QFLOW(I,J), HEAD(I,J), POWER(I,J), EFF(I), and RPM(J). Here the index I denotes a point in the original performance curve, and the index J identifies the speed. For constant head operation with variable speeds, the elements of the matrix HEAD(I,J) were searched to identify the intervals ΔH where the constant-head value fell, and linear interpolation was then used to calculate the other operational parameters.

These calculations were performed for the axial turbines A_1 and A_2, the axial pump P_1, and the Francis turbine F_3, at fixed gate. Similar calculations for operational conditions other than constant head H could also be performed by introducing the appropriate constraint in the matrices. Only constant head results are presented in this report, however.

Figure 5 shows the variable-speed characteristics of the axial-flow turbine A_1 (N_s=1.61), with fixed gate and blades, at constant head. It is seen that the discharge Q increases only slightly with the rotational speed, n. This means that operating the turbine at variable speed will not greatly facilitate flow control. Figures 6 and 7 present the corresponding characteristics for turbine A_2 and the axial-flow pump P_1 used as turbine. (For turbine A_2, a peak efficiency value $\hat{\eta} = 0.9$ was assumed in the calculations.) In both cases, there is a steeper rise of the curve of discharge versus rotational speed, which will be discussed further in section V. Figure 8 gives a comparison of variable-speed off-design performance curves for turbines A_1, A_2, and P_1. The corresponding curve for a full Kaplan, constant-speed turbine is also included. The coordinates are percent of peak efficiency and percent of peak-efficiency discharge to facilitate the comparison. The larger variation in discharge

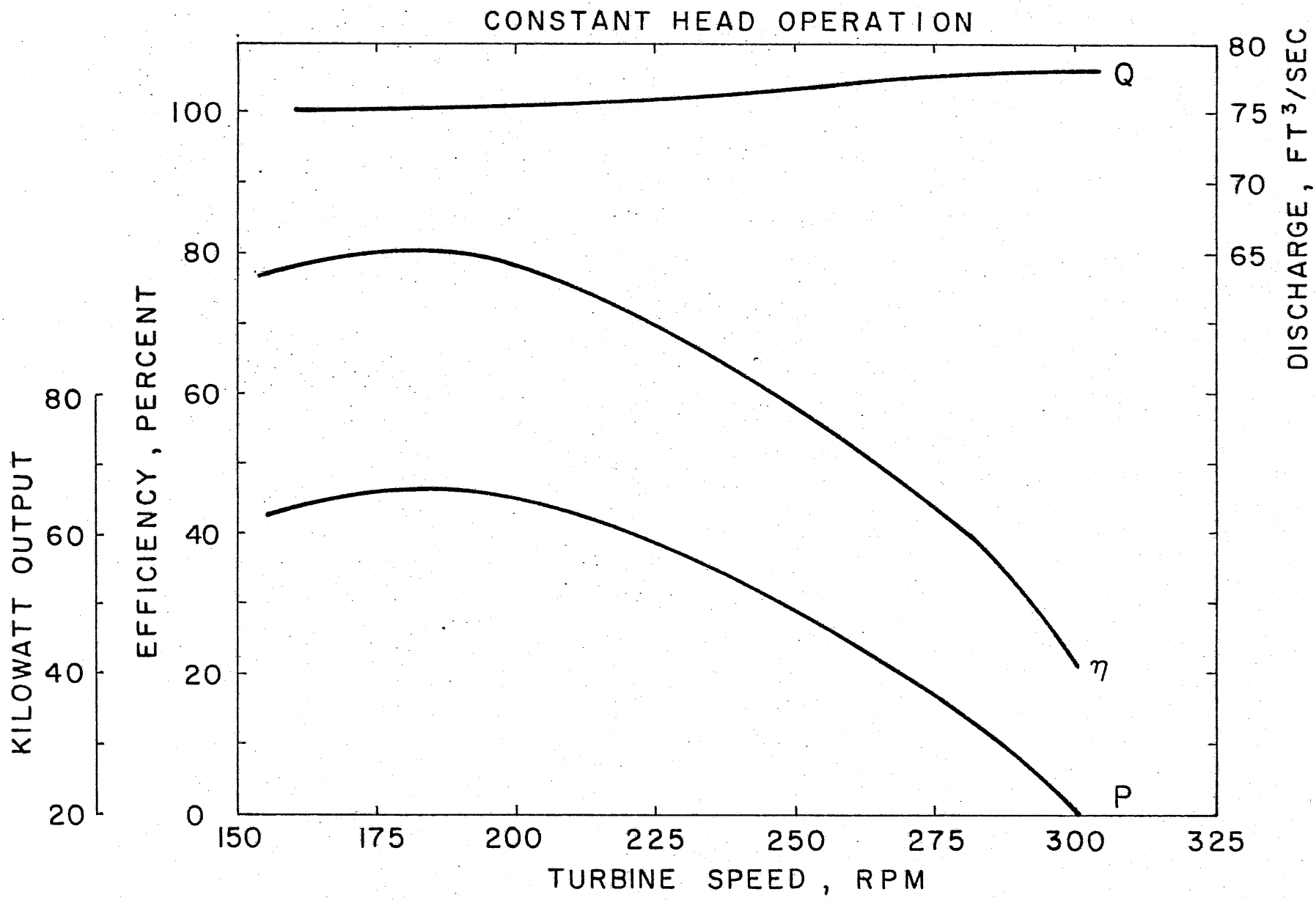

Fig. 5. Variable speed characteristics for axial-flow turbine A_1 (N_s = 1.61, fixed gate and blades.

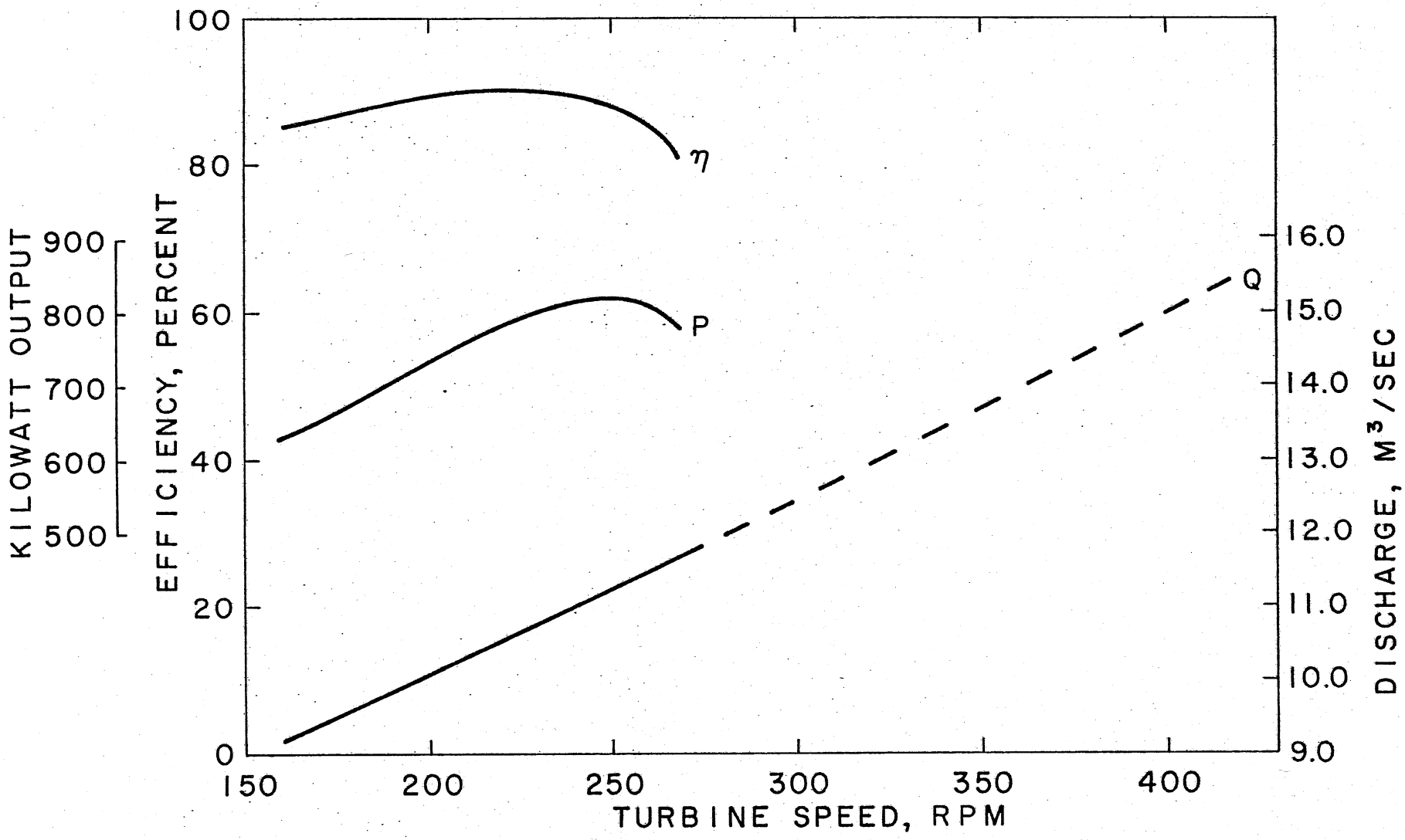

Fig. 6. Variable speed characteristics for axial-flow turbine A_2 (N_s = 2.65, fixed gate and blades).

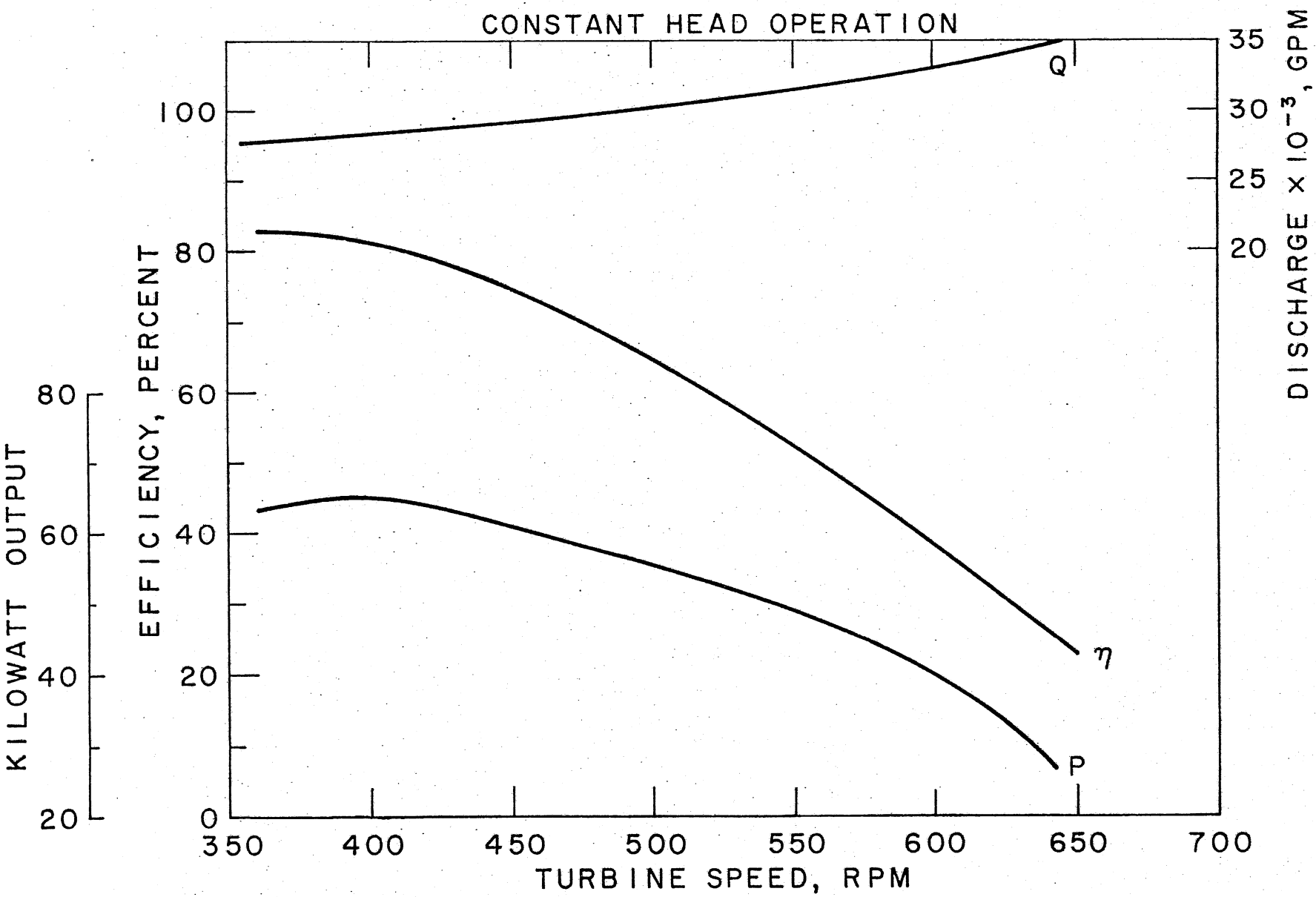

Fig. 7. Variable speed characteristics for axial-flow pump used as turbine (N_s = 2.68, fixed gate and blades).

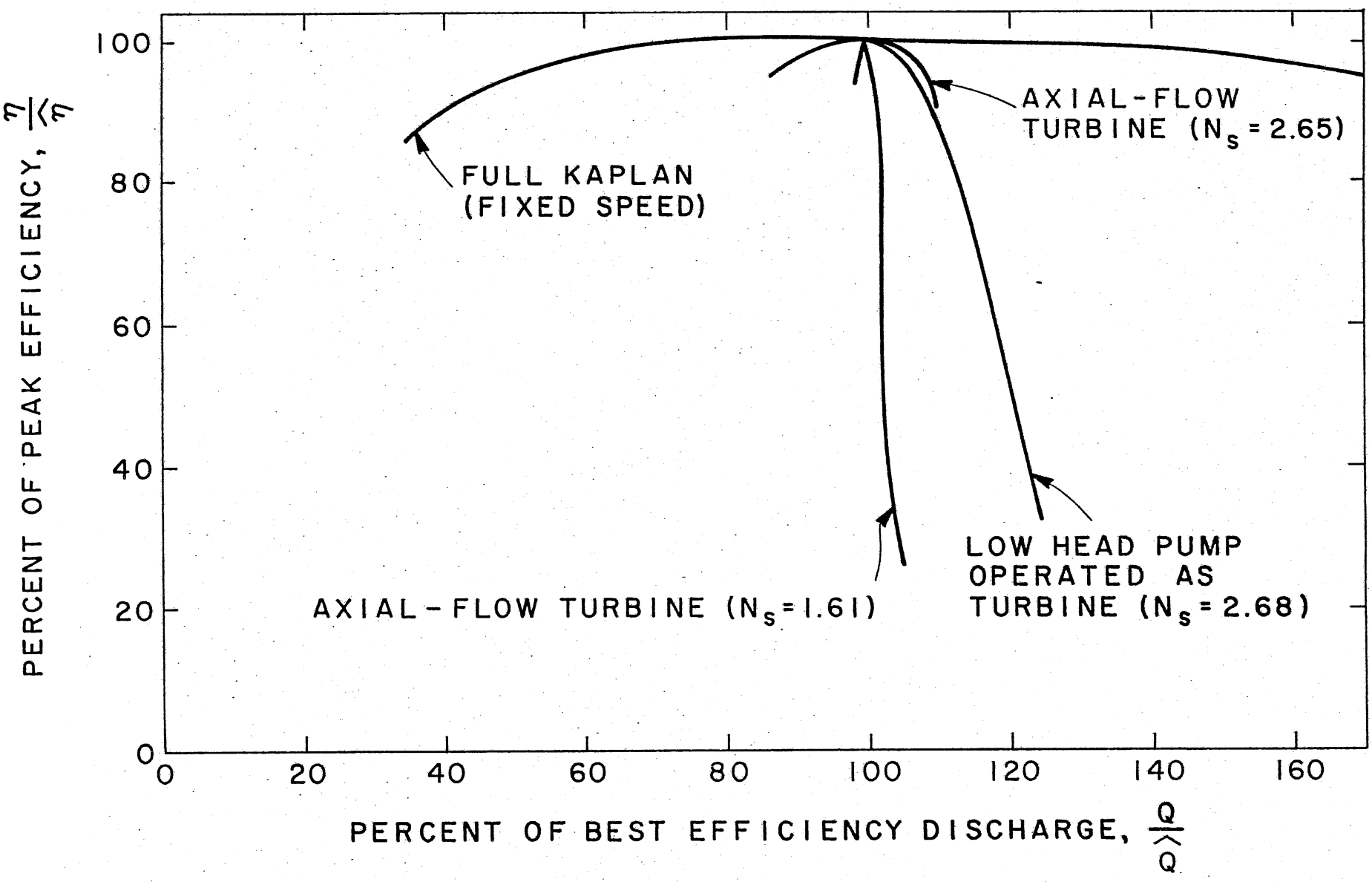

Fig. 8. Off-design variable-speed performance of fixed-gate, fixed-blade propeller turbines A_1, A_2, and P_1. Constant-speed Kaplan curve also shown for comparison.

obtained with turbines A_2 and P_1 in relation to that for turbine A_1 for which Q varies only slightly with n) is clearly exhibited in this figure. This may be related to the higher specific speed of turbines A_2 and P_1. Figure 8 indicates that the performance information supplied by the manufacturers, related to fixed-speed operation, is not sufficiently comprehensive to compute the full range of variable speed performance. At best, turbines A_2 and P_1 indicate a ± 20 percent range in turbine discharge with acceptable performance, which is much less than that which is achieved by fixed vane, variable-pitch blade turbines operating at constant rotational speed. This operational range, however, may be greater in higher specific speed turbines.

Now let us consider variable speed operation with a variable-gate capability, such as turbines F_1, F_2, F_3, and K_1. Points lying along the constant efficiency contours sketched in Fig. 9 represent different combinations of H,Q values for constant speed, n_o, and different gate openings. Given any such contour, say $\eta = \eta_A$, it is possible to obtain the smallest discharge, Q_B, such that for constant head H_B (taken equal to the best-efficiency head in Fig. 9), the efficiency η_A can be achieved for $Q = Q_B$ but not for any $Q < Q_B$. This is simply done by following the similarity parabola (passing through the origin) tangent to the contour $\eta = \eta_A$ from H_A to H_B. The speed, n_B, is given by $n_B = n_A(H_B/H_A)^2$. The discharge Q_B may be read from Fig. 9 or determined from the equation $Q_B = Q_A\, n_B/n_A$ (see Eq. 7). In practice, this was done by applying the similarity laws to all points on the curve $\eta = \eta_A$ and finding the homologous values for $H = H_B$. Point B then corresponds to the minimum value of Q computed from the contour $\eta = \eta_A$.

The performance curves for the Francis turbines analyzed herein were obtained from Bureau of Reclamation Monograph 20 (1976). For turbine F_3, Fig. 33 of this reference shows typical head-discharge hill curves for a range of N_s values (n_s = 48 to 75 in English units). An average value of $n_s = 62$ is assumed herein. Figure 10 shows the results for a fixed gate opening equal to 0.82 using the same procedure that was applied to the data for turbines A_1, A_2, and P_1. It is seen that Q is now a decreasing function of n.

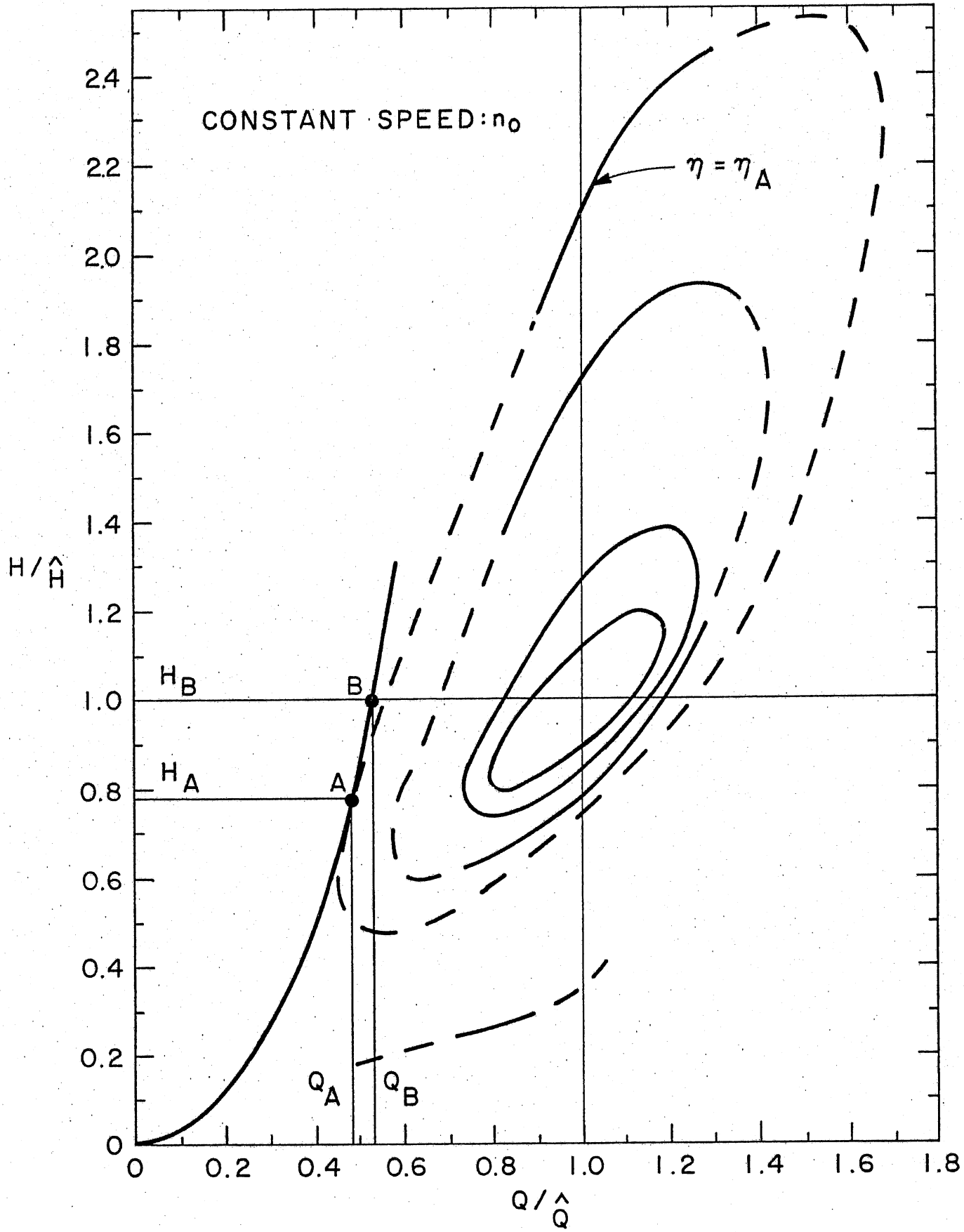

Fig. 9. Variable-gate characteristic curves on $H/\hat{H} - Q/\hat{Q}$ plane ($\hat{H}$, $\hat{Q}$: best efficiency values).

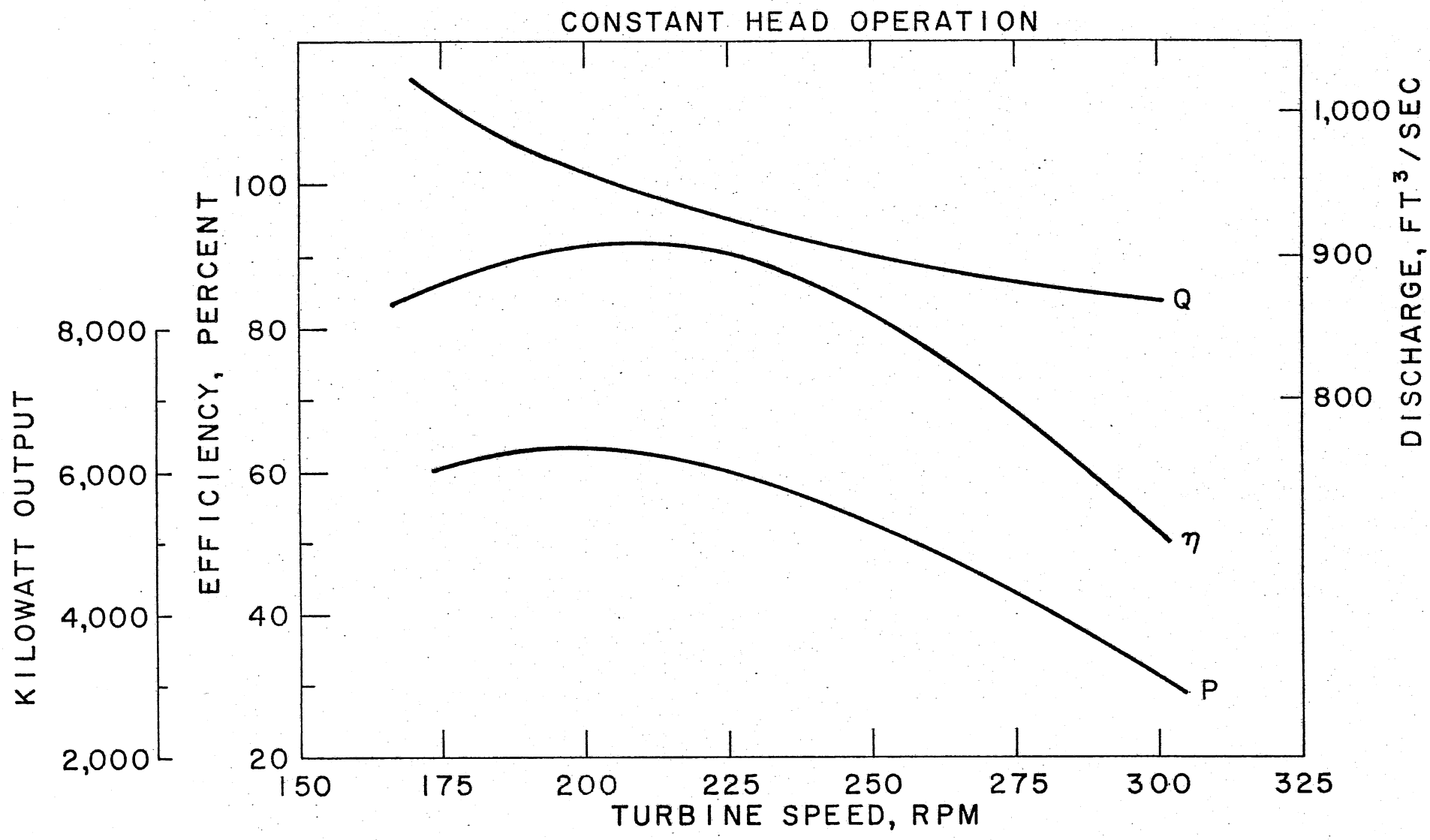

Fig. 10. Variable speed characteristics of Francis turbine F_3 (N_s = 1.43, fixed gate).

This result agrees with the calculations of Sheldon (1983), who found also a decrease in Q with increasing n for three Francis turbines with n_s values (in English units) of 24.5, 44.7, and 56.1. Actually, Sheldon's results show a trend toward smaller variations in Q with n with increasing n_s: the turbine with $n_s = 56.1$ exhibited practically no change in Q with an increase in rotational speed from 100 rpm to 160 rpm, while the unit with $n_s = 24.5$ exhibited a change in unit discharge from 0.85 cfs to about 0.55 cfs for a change in speed from 60 rpm to 130 rpm.

For turbines with variable gate, the procedure outlined in the preceding paragraph is of more interest, since one would want to use the variable gate capability along with variable speed. The results obtained for the three Francis turbines F_1, F_2, and F_3, and for the Kaplan turbine, K_1, are summarized in Table 1. No curves are presented because the differences are small, as can be seen from the Table. This indicates that the variable speed capability would not significantly improve the performance of these turbines at off-design flow and constant head.

TABLE 1. Comparison of Turbine Efficiencies for Fixed and Variable Rotational Speeds

Turbine	F_1	F_2	F_3	K_1
At $\frac{Q}{\hat{Q}}$ = 0.2		$\eta_{\text{var speed}}/\eta_{\text{fixed speed}}$		
= 0.4	74.0/74.0	75.1/75.0		83.8/83.5
= 0.6	85.3/85.0	83.7/83.2	82.0/81.3	90.5/90.0
= 0.8	91.2/91.0	89.5/89.2	89.3/88.9	91.5/91.0
= 1.0	92.2/92.2	92.0/92.0	92.0/92.0	92.0/92.0
= 1.2	86.0/86.0	90.1/90.1	89.8/89.8	91.5/91.5

Finally, the same variable-gate procedure was applied to a Bureau of Reclamation pump turbine (1977), T_1. The results are shown in Figs. 11 and 12. It is seen that Q is now an increasing function of n in both the turbining and pumping modes. There is significant improvement in turbine

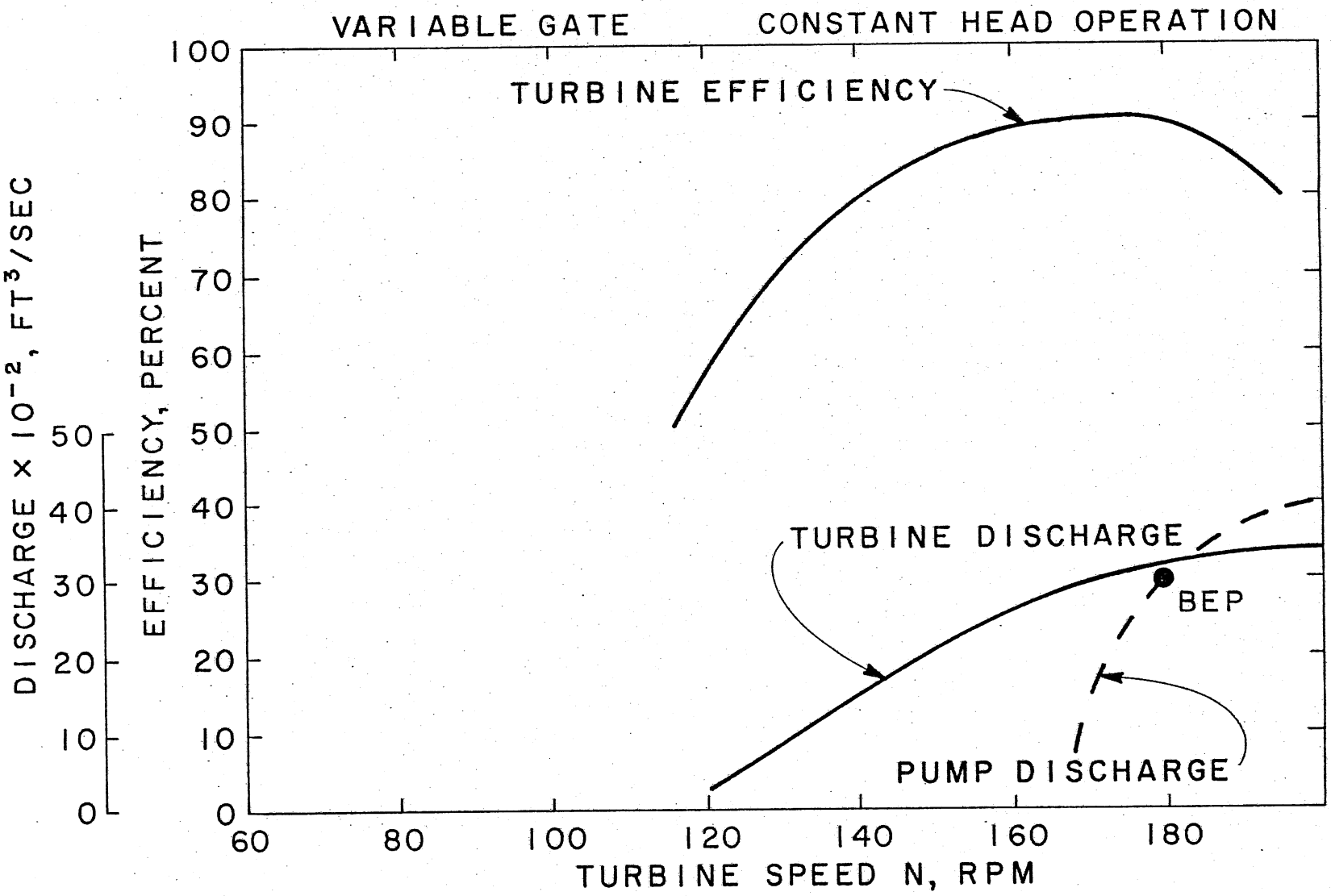

Fig. 11. Variable-speed characteristics of USBR pump turbine T_1 (N_s = 0.76).

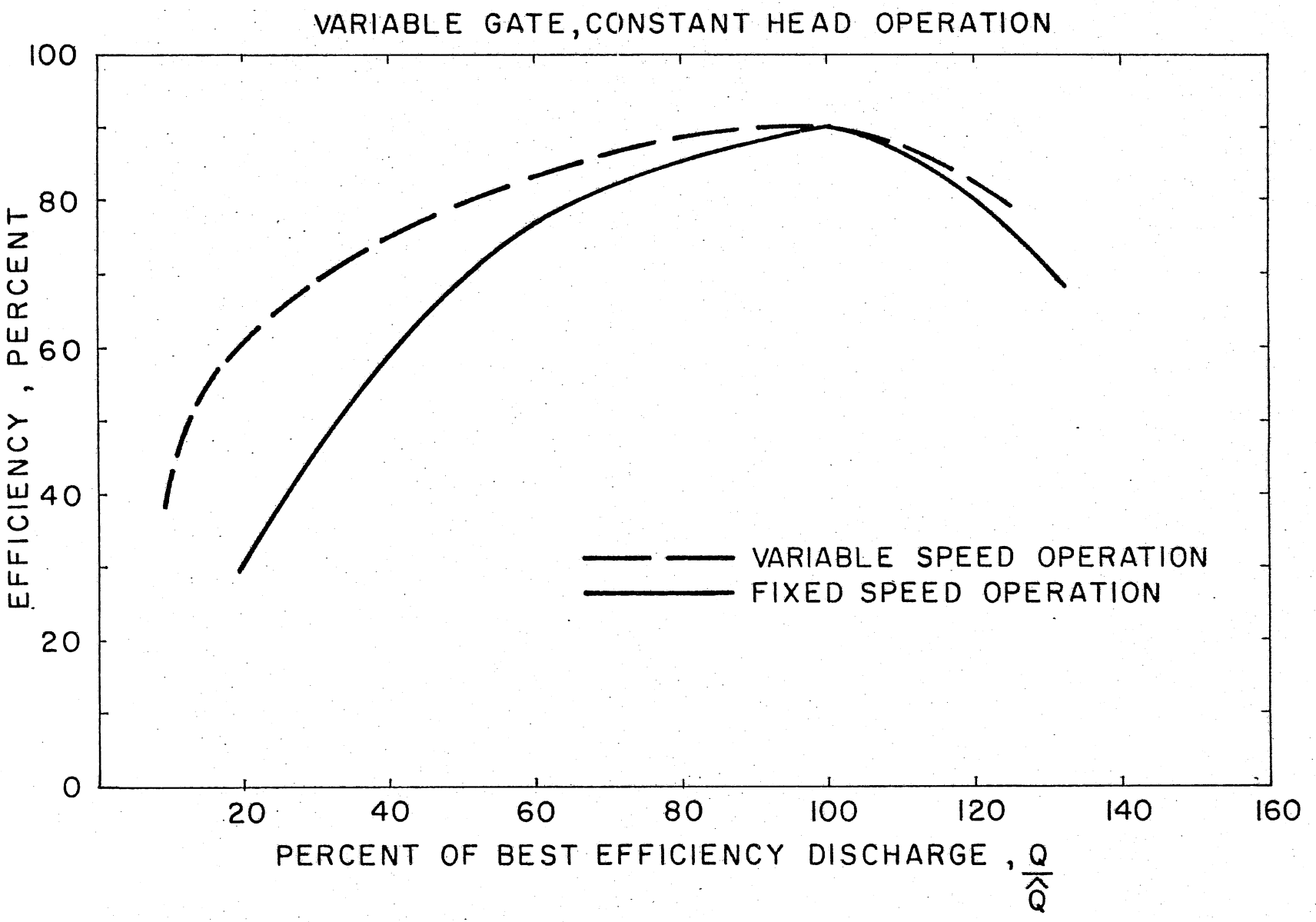

Fig. 12. Variable and fixed-speed characteristics of USBR pump turbine T_1 (N_s = 0.76).

efficiency at off-design flow and constant head, even though the specific speed of the unit is similar to turbine F_2, which experienced a very limited efficiency improvement. The authors are not certain as to the reason for this difference in results between units F_2 and T_1. Two possible reasons are:

1) That geometric shape of a pump-turbine runner is much closer to that of a pump than a turbine. Units F_2 and T_1 are therefore likely to be asimilar geometries.

2) The pump-turbine unit may not have been designed for off-design discharge at constant head, which would result in a very poor constant speed efficiency curve.

V. SOME THEORETICAL CALCULATIONS

The calculations in Section IV indicate that for constant H, the discharge (Q) appears to be a decreasing function of rotational speed (n) at low specific speed (N_s) (Francis turbines), while for larger N_s (axial-flow turbines) Q increases wtih increasing n. Within each turbine type this behavior depends on the characteristics of the individual machines, so it may be possible to have different Q versus n relationships for the same value of N_s, depending on the specific design. In other words, one may be able to influence the speed dependence by suitable design modifications. In this section, we examine briefly this problem in the case of axial-flow turbines, for which a relationship $Q(n)$ can be derived theoretically on the basis of certain parameters characterizing the blade lattice geometry.

To introduce the calculations, we look first at the case of a reaction turbine (not necessarily of the axial-flow type) with a sufficient number of blades so that the direction of the fluid flow at the exit from the runner is tangential to the exit blade angle. We write Euler's equation in the form

$$(gH)\eta_h = u_1 V_1 \cos \alpha_1 - u_2 V_2 \cos \alpha_2 \qquad (8)$$

where H is the turbine net head, g is the acceleration of gravity, η_h is the turbine hydraulic efficiency, the subscripts 1 and 2 denote inlet to exit from the runner, respectively, $\vec{V}$ is the fluid velocity and V its magnitude, α is the angle that the velocity vector $\vec{V}$ makes with the rotational velocity $\vec{u}$, and u is the magnitude of $\vec{u}$. In the space between distributor exit and runner inlet, one has, with sufficient approximation,

$$V_1 \cos \alpha_1 r_1 = V_0 \cos \alpha_0 r_0$$

where r is radial distance and the subscript 0 denotes exit from the distributor. We have, furthermore,

$$Q = V_0 \sin \alpha_0 (2\pi r_0) b_0$$

where b_0 is the channel width. Thus,

$$V_1 \cos \alpha_1 = \frac{Q}{2\pi b_0 r_1} \frac{1}{\tan \alpha_0} .$$

Then from the exit velocity triangle, one obtains

$$V_2 \cos \alpha_2 = u_2 - \frac{Q}{A_2} \frac{1}{\tan \beta_2}$$

where β_2 is the angle that the runner blades make with the negative $\vec{u}_2$ direction, and A_2 is the exit flow cross-sectional area. Combining Eq. (8) and the last two equations, one gets,

$$Q = \frac{r_2\Omega + \frac{\eta_h gH}{r_2 \Omega}}{\frac{1}{2\pi b_0 r_2} \frac{1}{\tan \alpha_0} + \frac{1}{A_2} \frac{1}{\tan \beta_2}} \qquad (9)$$

where Ω = rotational speed (rad/sec) = u/r.

This equation shows that under the conditions stated, the dependence of Q on n is of the form $An + B\eta_h/n$, where A and B are constants. If η_h were constant when n varies (which it is not), the $Q(n)$ graph would be of the form of the curve labeled "Eq. (14)" in Fig. 13. The minimum of the curve occurs in this case where $(r_2\Omega_{min})^2 = \eta_h(gH)$, that is $(\Omega_{min}/\Omega_{peak})^2 = \eta_h(gH)/(r_2^2\Omega_{peak}^2)$, with Ω_{peak} = best-efficiency or design speed. Depending on the value of the parameter $gH/(r_2^2\Omega_{peak}^2)$ (that is, of the parameter gH/n^2D^2, with $n = n_{peak}$), the design point could be to the right or left of the minimum, thus implying an ascending or descending $Q(n)$ curve. In practice, η_h varies with n, and the actual $Q(n)$ curve will depend on the type of turbine and the characteristics of the specific design.

V.1. Axial-Flow Turbines

The above analysis is not applicable to axial-flow turbines because the exit fluid angle from the runner is not generally equal to β_2. In the calculation that follows, this angle is first determined on the basis of the blade lattice parameters. The presentation is kept brief and only the major resulting equations are given here.

Consider a cylindrical section of the turbine of diameter $d = \sigma D$, where D is the runner diameter ($\sigma < 1$). For this cylindrical section, let t be the blade spacing in the lattice, ℓ the blade chord length, $\vec{v}$ the relative velocity and v its modulus, β the angle that the relative velocity vector makes with the negative $\vec{u}$ direction, $\vec{v}_\infty = (\vec{v}_1 + \vec{v}_2)/2$, and $v_a = v_{a_1} = v_{a_\infty}$ the axial or meridional flow velocity. The subscripts 1 and 2 again represent the inlet and outlet of the runner, respectively. If we assume irrotational flow, the magnitude of the lift force F_L on each blade is given by

$$F_L = \rho v_\infty \Gamma \tag{10}$$

where Γ is the circulation around each blade in the lattice, given by

$$\Gamma = t(v_2 \cos\beta_2 - v_1 \cos\beta_1)$$

Using superposition, one can show that Γ can be expressed in terms of the zero-lift-angle, β_0, for the lattice, and a dimensionless parameter δ, in the form:

$$\frac{\Gamma}{v_\infty t} = 2\delta \frac{\sin(\beta_\infty - \beta_0)}{\sin \beta_0} \tag{11}$$

The parameter δ represents the extent to which the relative fluid velocity leaves the runner at the runner's exit angle. Combining the last two equations, one obtains

$$v_2 \cos \beta_2 = v_1 \cos \beta_1 \frac{1 - \delta}{1 + \delta} + v_a \frac{2\delta}{1 + \delta} \frac{1}{\tan\beta_0}$$

This equation allows all components in the exit velocity triangle to be expressed in terms of inlet quantities, specifically in terms of v_a and α_1. One has in particular

$$V_1 \cos \alpha_1 - V_2 \cos \alpha_2 = \frac{2\delta}{1+\delta} \left(\frac{v_a}{\tan \alpha_1} - u + \frac{v_a}{\tan \beta_0} \right)$$

and Euler's Eq. (8) then yields (with $u_1 = u_2 = u$)

$$v_a \left(\frac{1}{\tan \alpha_1} + \frac{1}{\tan \beta_0} \right) = \frac{1+\delta}{2\delta} (g\eta_h H) \frac{1}{u} + u \qquad (12)$$

Assuming a uniform velocity distribution over the turbine cross section of external diameter D and hub diameter d_h, one has

$$Q = \frac{\pi}{4} (D^2 - d_h^2) v_a \qquad (13)$$

Introducing $u = \bar{r}\Omega$, where $\bar{r}$ is the radius of the characteristic cylindrical section considered, and replacing v_a from Eq. (13), one obtains, finally, from Eq. (12)

$$Q = \frac{\pi D^2}{4} \left(1 - \frac{d_h^2}{D^2}\right) \frac{\bar{r}\Omega + \frac{1+\delta}{2\delta} \eta_h (gH) \frac{1}{\bar{r}\Omega}}{\frac{1}{\tan \alpha_1} + \frac{1}{\tan \beta_0}} \qquad (14)$$

This equation differs from Eq. (9) mainly in the presence of the factor $(1+\delta)/2\delta$ in the second term in the numerator, where δ is the lattice parameter defined earlier.

An alternative derivation of Eq. (14) can also be given on the basis of the head-correction factor C_H as defined for example in Wislicenus (1965). Euler's Eq. (8) with $u_1 = u_2 = u$ is written in the form

$$(gH)\eta_h = C_H \, u (V_1 \cos \alpha_1 - V_2^* \cos \alpha_2^*) \qquad (15)$$

where the absolute velocity vector $\vec{V}_2^*$ is that which would be obtained if the flow left the blade in the direction of zero lift, α_2^* is the angle this vector makes with the $\vec{u}$ direction, and C_H is the correction factor

needed to make the righ-hand sides of Eqs. (8) and (15) equal. One can then show that on the basis of C_H as defined by Eq. (15), the same Eq. (14) is obtained with $2\delta/(1+\delta)$ replaced by C_H.

V.2. Estimation of the Lattice Parameter δ

In order to apply Eq. (14) to an actual turbine it is necessary to estimate the lattice parameters δ (or $C_H = 2\delta/(1+\delta)$) and β_0. For thin profiles with small mean-line curvatures, one can use as a first approximation theoretical results available for a lattice of flat plates of length L and spacing s, inclined at an angle β_0 relative to the negative u direction. The lift coefficient for a plate in such a blade system is given by (Durand, 1935)

$$C_L = 2\pi K \sin\alpha \tag{16}$$

where α is the angle of attack and K is a factor that depends on the lattice geometry, that is, a function of $\sigma = \ell/t$ (chord length divided by the spacing) and the angle β_0. Here, C_L is defined by

$$F_L = C_L \tfrac{1}{2}\rho v_\infty^2 \ell \tag{17}$$

where F_L is the lift force per unit width and ρ the mass density of the fluid. Combining Eqs. (17) and (10) one has also

$$\Gamma = \tfrac{1}{2} C_L v_\infty \ell \tag{18}$$

and therefore the parameter δ defined by Eq. (11) can be calculated from the results for the lift coefficient. One obtains

$$\delta = \frac{\pi\ell}{2t} \sin\beta_0 \, K\left(\frac{\ell}{t}, \beta_0\right). \tag{19}$$

Likewise,

$$C_H = \frac{2}{1 + \dfrac{2t}{\pi\ell} \dfrac{1}{\sin\beta_0} \dfrac{1}{K}} \tag{20}$$

Graphs of δ and C_H as functions of β_0 and $\sigma = \ell/t$ are given respectively in Mataix (1975) and Wislicenus (1965).

V.3. Application to Axial-Flow Turbine A_2

Available information on design characteristics for the axial-flow turbine labeled A_2 in Table 1, Section IV, has been used to test Eq. (14). The information on hand was completed as needed, introducing suitable assumptions. Known parameters were: diameter D = 1.8 m, head $\hat{H}$ = 8.3 m, discharge $\hat{Q}$ = 10.65 m^3/s and speed $\hat{n}$ = 222 rpm ($\hat{H}$, $\hat{Q}$, and $\hat{n}$ are design or peak-efficiency values). The number of blades was z = 5. A peak efficiency $\hat{\eta}$ = 0.90 was assumed for the machine. Application of Eq. (14) required estimates of the hub diameter ratio d_h/D, the radius $\bar{r}$ of a typical cylindrical section, and the various dimensions and angles in the velocity triangles. These were obtained assuming that the absolute velocity vector at exit from the runner was perpendicular to the rotational velocity $\vec{u}$, that is, $V_2 \cos \alpha_2 = 0$, and using Euler's equation to calculate $V_1 \cos \alpha_1 - V_2 \cos \alpha_2 = V_1 \cos \alpha_1$. Since v_a is known from the known value of $\hat{Q}$ and the assumed hub-diameter ratio (see Eq. 13), the velocity triangles for the cylindrical section at $\bar{r}$ could be drawn. The blade spacing and chord length were estimated from the number of blades, the $\bar{r}$ value chosen, and available sketches of the turbine. Finally, Eq. (19) and Eq. (14), written for the best-efficiency point, were used to obtain reasonable estimates of β_0 and δ, taking into account the value of β_∞ as determined from the velocity triangles.

For the particular case of turbine A_2, the following equation resulted from these estimates

$$\frac{Q}{\hat{Q}} = 0.72 \frac{n}{\hat{n}} + 0.31 \eta_h \frac{\hat{n}}{n} \qquad (21)$$

The values of η_h for varying n were obtained from the available performance curves for this turbine. This equation is represented in Fig. 13. Also given in Fig. 13 are the curve resulting from the similarity calculations on turbine A_2 and a curve corresponding to Eq. (14), with the numerical values in Eq. (21), but with $\eta_h = 1.0$ for all n values.

Finally, a tentative calculation to show what would be the effect of varying certain characteristic design parameters of the turbine on the Q(n)

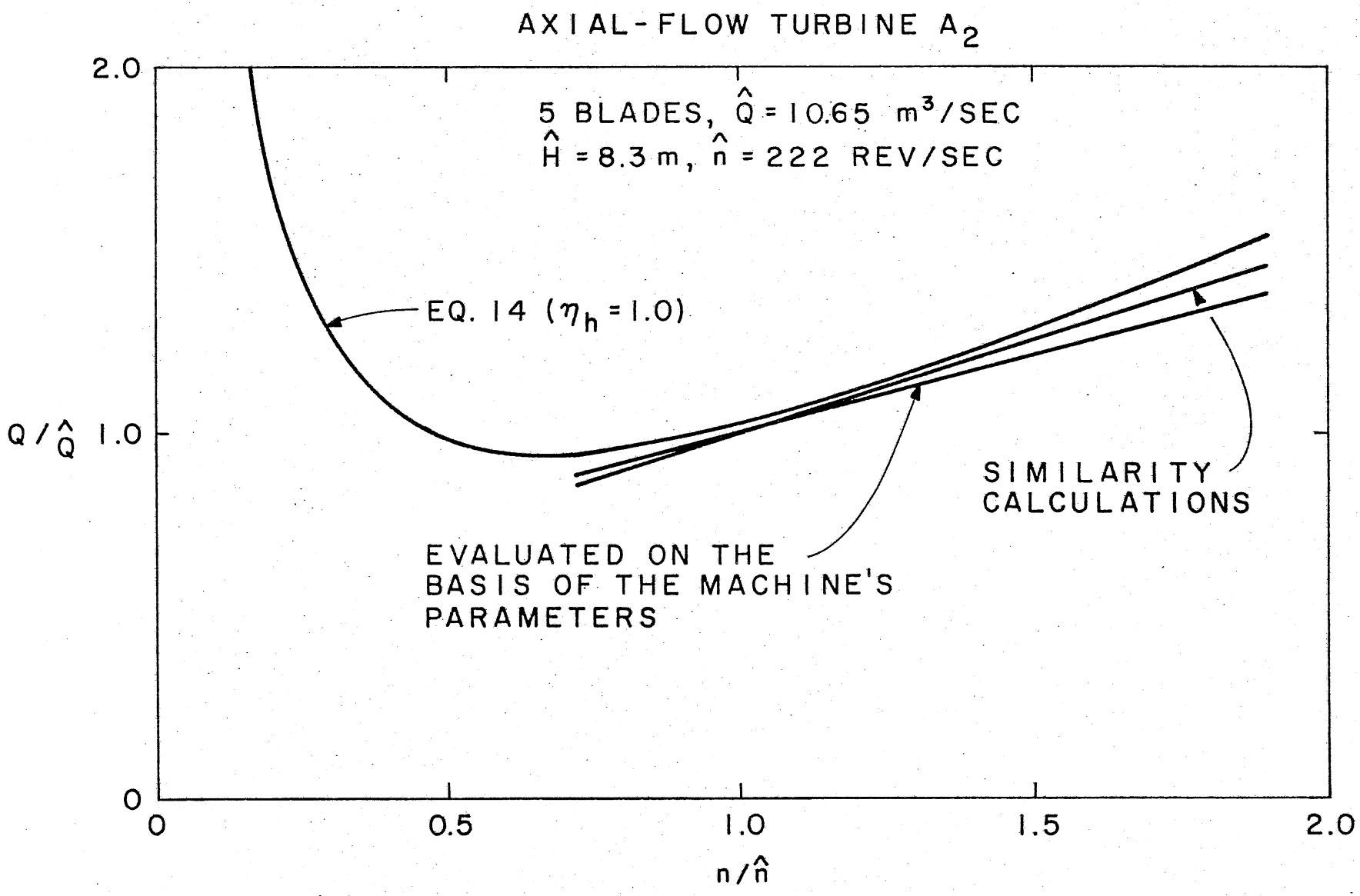

Fig. 13. Variation of turbine discharge versus rotational speed from measured performance characteristics and two analytical calculations (Eq. 14 and similarity calculations).

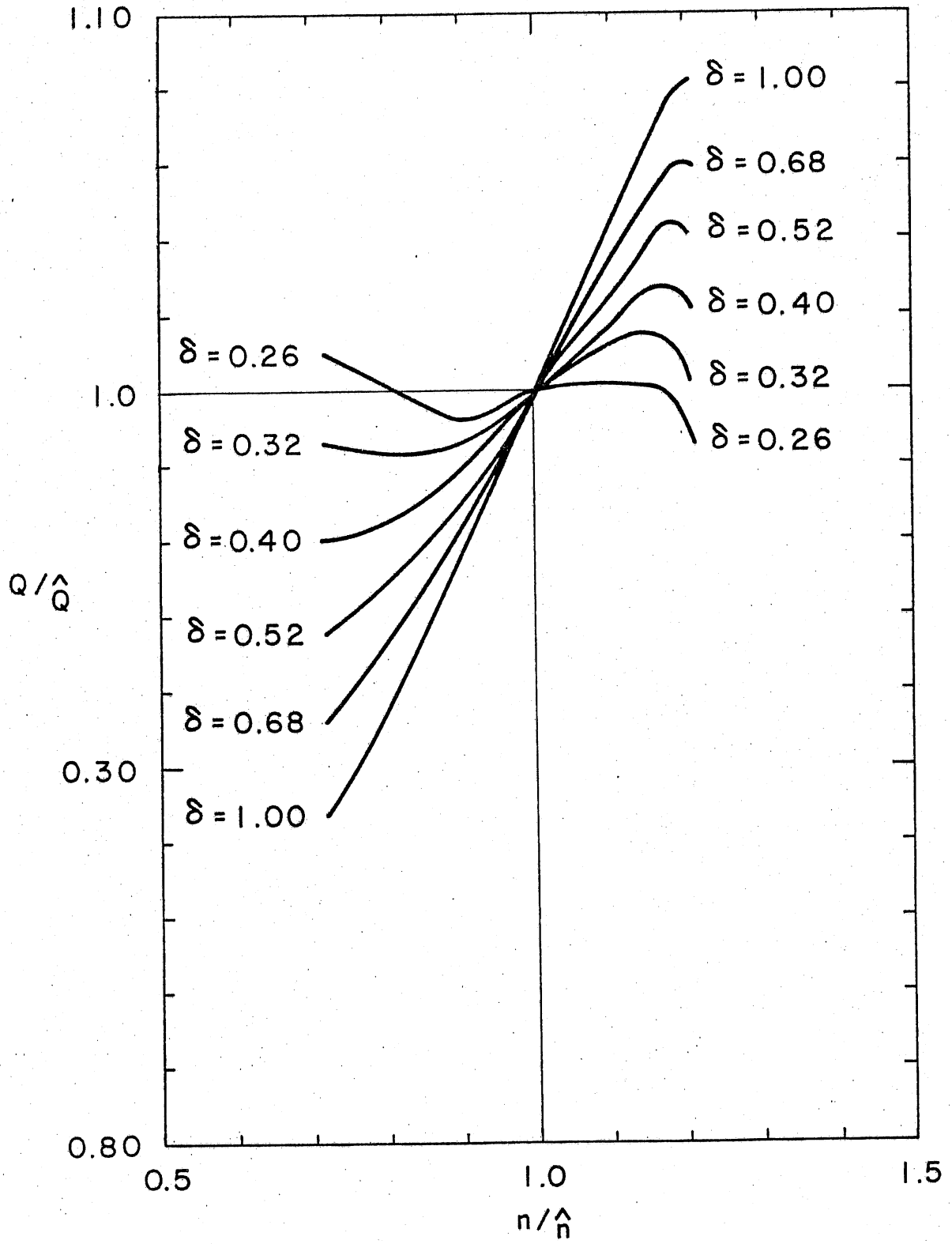

Fig. 14. Effect of parameter, δ, on the variation of turbine discharge with rotational speed. Determined from theoretical calculations.

dependence at constant H is presented in Fig. 14. The curves on this figure are parametric in the parameter δ defined by Eq. (11), and given by Eq. (19) for the case of a lattice of flat plate profiles. Essentially, the variation in δ must be accomplished, as shown by Eq. (19), through variations in the ratio $r = \ell/t$ or in the angle β_0. These results will be developed in more detail elsewhere.

VI. SUMMARY AND CONCLUSIONS

1. The hydromechanical aspects of variable-speed hydroturbine operation were investigated to estimate the potential improvement in performance associated with the variable speed capability.

2. The potential advantages of the variable-speed turbine are a) improved performance at off-design heads and improved range of operating head, b) improved performance at off-design discharge, and c) improved performance for pump-turbine units, where peak performance rotational speed may be different for the pumping and turbining modes.

3. Variable-speed performance diagrams at constant head for two small axial-flow turbines with fixed vanes and blades, an axial pump used as a turbine, three Francis turbines, a pump turbine, and a Kaplan turbine, were obtained from information supplied by manufacturers or available in the literature. These performance diagrams were used in conjunction with similarity laws to obtain the variable speed performance characteristics at constant head operation.

4. The calculations indicate a ± 20 percent range of turbine discharge at constant head, with acceptable performance, for one of the axial flow turbines with fixed vanes and blades and for the axial flow pump used as a turbine. No significant performance improvement was found for the other axial flow turbine. The turbines with a higher specific speed had the greatest improvement in performance.

5. The variable speed capability did not significantly improve the performance of the three Francis turbines at off-design discharge and constant head when used along with the variable-gate capability of these turbines. The same result was obtained for the Kaplan turbine.

6. A significant improvement in turbining efficiency at off-design flow and constant head was found for the pump-turbine, even though the specific speed of the unit is similar to one of the Francis turbines discussed above. Two possible reasons for this difference are:

   - o The geometric shape of a pump-turbine runner is much closer to that of a pump than a turbine. The two units are therefore likely to be asimilar geometries.
   - o The pump-turbine unit may not have been designed for off-design discharge at constant head, which would result in a very poor constant speed efficiency curve.

7. The dependence of turbine discharge, Q, on rotational speed, n, is shown theoretically to be of the form

$$Q = An + B\eta_h/n$$

   where A and B are constants, and η_h is the turbine hydraulic efficiency. This implies an ascending or descending Q versus n curve, depending upon whether the design point of the turbine is to the right or left of the minimum in the above equation. For axial-flow (propeller) units, it is shown how the parameters A and B depend on the design characteristics.

8. The theoretical calculations confirm the variations of Q with n at constant head for the propeller turbine exhibiting the largest $Q(n)$ changes. Furthermore, a tentative calculation is presented to show what the effect of varying certain characteristic design parameters of the turbine could be on the $Q(n)$ dependence at constant head.

9. Additional research on variable speed turbine hydromechanics is needed, on the one hand with more comprehensive data sets for existing turbines, on the other, to establish the feasibility of designing a turbine to achieve variable-speed characteristics of possible interest. Improvements in performance and ranges of application may be enhanced if a runner is specifically designed for variable-speed operation.

10. Diffuser performance for high specific speeds needs reevaluation. At high N_s diffuser efficiency is generally very important. The loss of efficiency of propeller units at off-design speeds may be offset by improved diffuser efficiency. For variable-speed turbines in particular, excess swirl results at exit from the runner, which may be used at least partly to improve diffuser performance.

11. Cavitation characteristics of turbines as functions of speed need also additional study. On a more general note, more model tests and turbine research need to be performed for the public domain.

VII. REFERENCES

1. Alexander, G. C., "A case study of Francis turbine variable-speed efficiency gain," presented at Workshop on Variable Speed Generators - Hydro Applications, Denver, Colorado, May 1983.

2. Arndt, R. E. A., Farell, C., and Wetzel, J., "Hydraulic turbines," in Small Hydropower Systems Design, McGraw-Hill (in press).

3. Department of Energy and Electric Power Research Institute, Workshop on Variable Speed Generators - Hydro Applications, Denver, Colorado, May 1983.

4. Durand, W. F., Aerodynamic Theory, Vol. 4, Berlin, 1935.

5. Mataix, C., Turbomáquinas Hidráulicas, Editorial Icai, Madrid, 1975.

6. Nair, R., "Development potential for low-head hydro," Water Power and Dam Construction, December, 1982, pp. 49-56.

7. Sheldon, L. H., "An analysis of the benefits to be gained by using variable speed generators on Francis turbines," presented at Workshop on Variable Speed Generators - Hydro Applications, Denver, Colorado, May 1983.

8. Stelzer, R. S. and Walters, R. N., "Estimating reversible pump-turbine characteristics," Engineering Monograph No. 39, Bureau of Reclamation, December 1977.

9. United States Bureau of Reclamation, "Selecting hydraulic reaction turbines," Engineering Monograph No. 20, 1976.

10. Wislicenus, G. F., Fluid Mechanics of Turbomachinery, Vol. 1, Dover Publications, Inc., New York, 2nd Ed., 1965.

11. Wislicenus, G. F., "Hydrodynamic machinery," in Fluid Mechanics Research in Water Resources Engineering, Proceedings, 40th Anniversary Symposium, R.E.A. Arndt and M. March, ed., St. Anthony Falls Hydraulic Laboratory, Dept. of Civil and Mineral Engineering, Univ. of Minnesota, Minneapolis, MN, April 1979.